Joint International Topical Meeting on Mathematics & Computation and Supercomputing in Nuclear Applications (M&C + SNA 2007)
Monterey, California, April 15-19, 2007, on CD-ROM, American Nuclear Society, LaGrange Park, IL (2007)

ENERGETIC, KINETIC AND CRYSTALLOGRAPHIC CHARACTERISTICS OF SELF-POINT DEFECTS IN VANADIUM AND IRON CRYSTALS

A.B. Sivak and V.M. Chernov
A.A. Bochvar Institute of Inorganic Materials
123060, P.O. Box 369, Moscow, Russia
chernovv@bochvar.ru

V.A. Romanov
A.I. Leipunsky Institute of Physics and Power Engineering
249033, Bondarenko sq. 1, Obninsk, Russia
romanov-ippe@mail.ru

ABSTRACT

In bcc V and Fe crystals, the study of formation and migration mechanisms, energetic and crystallographic characteristics of self-point defects (self interstitial atom, vacancy) has been carried out by molecular statics and molecular dynamics methods with use of semiempirical many body interaction potentials.

Key Words: vanadium, iron, self-point defects, diffusion, interatomic interaction potentials

1. INTRODUCTION

Predictive ability of phenomenological models of changes of material macroproperties depends critically on the reliability of knowledge of self-point defects (vacancies and SIAs – self-interstitial atoms) characteristics and their clusters. There are significant difficulties in determining self-point defects characteristics by experimental methods. Therefore the problem of development and refinement of theoretical methods of investigation of self-point defects behavior and their interaction with other crystal lattice defects (dislocations, others) is of importance.

Until now alternative models, suggested for the description of self-defects behavior in iron and vanadium, are discussed in literature. The situation concerning iron was analyzed in detail in [1] and it was shown that the vacancy migration took place at the annealing stage III of irradiated high purity iron at temperature ~ 270 K.

The properties of self-point defects in vanadium are much less investigated by experimental and theoretical methods. Due to this there are two practically equally justified points of view regarding the behavior of self-defects in this metal. The authors of [2,3] proves the point of view that the vacancy migration energy in vanadium equals to (1 – 1.3) eV basing on the results of measurements of self diffusion and equilibrium vacancy concentration by positron annihilation technique. Essential drawback of this model is that the influence of interstitial impurity atoms

forming stable complexes with vacancies was not taken into account. Alternative approach [4,5] is based on the analysis of annealing stages of irradiated vanadium was suggested. In this case the vacancy migration takes place at the temperature of the annealing stage III (170 K – 200 K) and is characterized by the activation energy (0.4 – 0.5) eV. There is even more uncertain situation regarding the symmetry and the migration energy of the stable SIA configuration in vanadium. *Ab initio* calculations [6,7] predict stability of <111> dumbbell SIA configuration in V and other bcc refractory metals (except for Fe) and very low SIA migration energy. However, the results regarding the symmetry and mobility of SIA in Mo and W contradict to experimental observations [8]. It is possible that this discrepancy is the consequence of approximations employed in *ab initio* calculations. The analysis of experimental data [5,9-12], taking into account the influence of solute interstitial impurity on the annealing kinetics, drew to a conclusion [13] that the vacancy migration takes place at the annealing stage III, and the migration of the stable SIA configuration takes place at the annealing stage I_E (~ 80 K) with the activation energy ~ 0.2 eV.

In this work the results of study of self-point defect characteristics by molecular statics (MS) and molecular dynamics (MD) in Fe and V crystals are presented. Calculations were performed on the base of suggested interatomic potentials [1,13] developed with the condition of the best agreement of the complex of calculated defects characteristics and the corresponding experimental data set.

2. INTERATOMIC POTENTIALS IN VANADIUM AND IRON CRYSTALS

Interatomic interaction potential [13] describing interactions in vanadium crystal was developed by using Finnis-Sinclair approach [14]. In the framework of this method the total energy E of the system containing N atoms can be written as

$$E = \frac{1}{2}\sum_{i=1, i\neq j}^{N} \varphi\left(r_{ij}\right) - \sum_{i=1}^{N}\left[\sum_{j=1, j\neq i}^{N} \rho\left(r_{ij}\right)\right]^{1/2}, \qquad (1)$$

where $\varphi(r)$ and $\rho(r)$ are the empirical functions describing pairwise and many body interactions in the crystallite; r_{ij} is the distance between atoms i and j.

The functional dependence $\rho(r)$ at $r < r_2$ (r_k is the distance to the k^{th} nearest neighbor in bcc lattice) was written as

$$\rho\left(r\right) = \left[a\left(r - r_C\right)^n + b\left(r - r_C\right)^m\right], \qquad (2)$$

where n, m ($n < m$) are the integer variables, r_C is the cutoff distance, and values a, b are determined analogously to algorithm [14]. $\rho(r)$ consists of two 5^{th} order polynomials at $r_2 < r < r_C$. Their coefficients were determined from the condition of joining of the polynomials and their first three derivatives with each other and with the function (2) at $r = r_i$ at $r = r_2$, correspondingly, and the condition that $\rho(r)$ and its first three derivatives were equal to zero at $r = r_C$.

Pair potential $\varphi(r)$ consists of the set of 5th order polynomials joined to the third derivative. The condition of joining of $\varphi(r)$ and its first three derivatives with the universal screening Coulomb potential [15] at short distances and the condition that $\varphi(r)$ and its first three derivatives were equal to zero at $r = r_C$ were used.

The following experimental data set of vanadium bulk properties was used for determination of potential parameters: lattice constant r_2 = 0.30204 nm at zero temperature; the elastic constants $c_{11} = 238.2$ GPa, $c_{12} = 122.04$ GPa, $c_{44} = 46.8$ GPa [16]; the sublimation energy $E_S = 5.30$ eV [17]; the equation of state $P(V)$ [18,19]. Under the condition of the maximal satisfaction to this experimental data set, ultimate parameters of functions $\varphi(r)$ and $\rho(r)$ were determined by an iteration method during the process of adjustment of calculated values of the vacancy formation E_V^F and migration energies E_V^M, SIA migration energy E_I^M to the corresponding values chosen on the basis of the analysis of experimental data complex. As a result of this analysis of the experimental data on the annealing stages of irradiated specimens [9-11], self diffusivity [20-25], thermally equilibrium vacancy concentration measured by the positron annihilation method [2,3], kinetics of dislocation loop concentration change under the irradiation in the high-voltage electron microscope [12], kinetics of helium thermodesorption [5] and others, the following values of self-point defect characteristics in vanadium were extracted to which the computer model was adjusted: $E_V^F = (2.55 \pm 0.05)$ eV; $E_V^M = (0.45 \pm 0.05)$ eV; $E_I^M = (0.18 \pm 0.03)$ eV. Tables A.I –A.III list the obtained parameters of the functions $\varphi(r)$ and $\rho(r)$.

The semi-empirical model of transition metal [1] used for studying defects in iron crystal describes the ion core interactions in the framework of pair central-symmetric interaction potential and takes into account effects of electron density redistribution under crystal distortion or defect formation by introducing a volume dependent additive component into the crystal energy density. Parameters of the functional dependence of the interaction potential were determined by the iteration method during the process of adjustment of model results to experimentally known bulk properties of the crystal and characteristics of self-defects. The model results precisely meet the equilibrium elastic constants and agree with experimental measurements of the equation of state, dispersion curves, Debye frequency, Gruneisen constant and temperature dependencies of thermal properties (lattice constant, temperature coefficient of linear expansion, thermal vibrations amplitude of atoms) [1].

3. COMPUTING METHODS OF SELF-POINT DEFECTS CHARACTERISTICS

To calculate the defect characteristics by MS, a cubic model crystallite under a fixed boundary condition containing $\sim 10^4$ free atoms was used. The model crystallite was composed of three areas: the inner area I, the intermediate area II and external area III. The atoms of the area I were free, and the atoms of the areas II and III were fixed. The area III was necessary to nullify the forces acting on the atoms of the area II in the perfect crystallite. The minimization of the potential energy of the crystallite containing a defect was performed by steepest descent method until the maximal acting force magnitude was greater than 10^{-6} eV/nm.

Calculation of the dipole tensor P_{ij} was performed using algorithms [26,1]:

$$P_{ij} = \sum_k x_i^k F_j^k \,, \tag{3}$$

where x_i^k are the Cartesian coordinates of the radius-vector $\vec{r}_k$ of the atom k belonging to the area II; F_j^k are the projections of the forces acting on the atom k after relaxation of the defect configuration in area I. Eq. (3) contains the summation over all the atoms of area II.

The relaxation volume of point defects was calculated with use of the relation [27]

$$V^R = TrP_{ij} \big/ \left(c_{11} + 2c_{12}\right). \tag{4}$$

The study of defect diffusion was carried out by MD using of the model crystallite with applied periodic boundary conditions. The model crystallite was microcanonical ensemble (constant number of atoms N, volume V and energy E). Lattice constant r_2 was chosen so that module of the pressure P was less than 0.1 eV/nm^3. The Verlet algorithm [28] was used for the integration of the equations of motions. The value of a time step was chosen so that the fastest atom displacement per one iteration was less than ~0.007 r_2. The crystallite consisted of (4394+1) and (2000–1) atoms in case of SIA and vacancy diffusion, correspondingly. The determination of the position of self-point defects was based on the analysis of number of atoms through all Wigner-Seitz cells. The crystallite centre was kept near the defect by reassignment of boundaries after each defect jump in conformity with the technique proposed in [29]. Simulation time amounted to ~ (2 – 600) ns depending on the temperature and defect type. At each considered temperature the total number of defect jumps was 10^4 and $2 \cdot 10^4$ for vacancy and SIA, correspondingly.

The defect diffusion coefficient D^d was calculated in conformity with algorithm [29,30]:

$$D^d = \frac{1}{N_S} \sum_{i=1}^{N_S} D_i = \frac{1}{N_S} \sum_{i=1}^{N_S} \frac{1}{n_i} \sum_{j=1}^{n_i} \frac{R_{i,j}^2}{6\tau_i}, \tag{5}$$

where N_S is the total number of series of trajectory decomposition to segments of an equal duration τ_i, n_i is the number of segments in the i^{th} series, $R_{i,j}$ is the magnitude of the defect displacement vector of the j^{th} segment in the i^{th} series. The analysis of the convergence of diffusivity and its statistical inaccuracy versus the number of segments revealed that the optimal ranges for n_i are $n_i \in [950,1050]$ for SIA and $n_i \in [1950,2050]$ for vacancy.

Tracer diffusion constant per one defect D^* was calculated using the Einstein equation for the case of 3D diffusion:

$$D^* = \frac{1}{c_d} \frac{\left\langle R^2(t) \right\rangle}{6t}, \tag{6}$$

where $\left\langle R^2(t) \right\rangle = \frac{1}{N} \sum_{i=1}^{N} \left[\vec{r}_i(t) - \vec{r}_i(0) \right]^2$ is the mean square displacement of the tracer atoms, N is

the number of atoms in the model crystallite (all the atoms were assigned as tracers), $\vec{r}_i(0)$ and $\vec{r}_i(t)$ are initial and instantaneous positions of atom i, $c_d = 1/N$ is defect concentration. Time t was taken equal to the total simulation time.

Defect correlation factor f_d was determined as the ratio of the diffusion constant D^d calculated by Eq. (5) to the diffusion constant D^{RW} calculated under the assumption of defect random walk (RW) [31]:

$$D^{RW} = \sum_i \frac{\nu_i \lambda_i^2}{6}, \tag{7}$$

where ν_i is the frequency of defect jumps with jump distance λ_i.

Tracer correlation factor f_{tr} was determined as the ratio of the tracer diffusion constant D^* to the defect diffusion constant D^d.

4. SELF-POINT DEFECTS CHARACTERISTICS IN VANADIUM AND IRON CRYSTALS

4.1. Vanadium

Table I lists the characteristics of various self-defects calculated by MS in V crystal. The vacancy formation and migration energies agree with the results of *ab initio* calculations (formation energy 2.60 eV [6] and 2.51 eV [7]; migration energy 0.33 eV [6] and 0.62 eV [7]). The stable SIA configuration is <110> dumbbell with the migration energy 0.17 eV. The formation energy of <111> dumbbell is higher than the one of <110> dumbbell by 0.15 eV. This result does not match with the results *ab initio* calculations [6,7] (<111> dumbbell is the stable SIA configuration). However it agrees well with the given above results of experimental data analysis.

Table I. Calculated formation E^F and migration E^M energies (eV), relaxation volume $V^R(\Omega)$ (Ω – atomic volume) and dipole tensor P_{ij} (eV) for self defects in V crystal

Defect configuration	E^F	E^M	V^R	P_{11}	P_{22}	P_{33}	P_{13}	P_{23}	P_{12}
<110> dumbbell	3.13	0.17	0.98	12.56	12.56	15.40	0	0	4.14
<110> dumbbell saddle point	3.30		1.07	14.62	15.32	14.62	2.96	0.80	2.96
<111> dumbbell	3.28	0.01	1.17	16.19	16.19	16.19	3.96	3.96	3.96
Vacancy	2.50	0.48	-0.16	-2.22	-2.22	-2.22	0	0	0
Vacancy saddle point	2.98		-0.28	-3.91	-3.91	-3.91	-0.75	-0.75	-0.75
Divacancy 2nd nn	4.72	0.52	-0.23						
The stable di-SIA	5.55	0.08	2.14						

4.2. BCC Iron

Table II lists the characteristics of various self-defects calculated by MS in Fe crystal. The vacancy formation and migration energies agree well with the experimental measurements (formation energy (2.0 ± 0.2) eV [32]; migration energy (0.73 ± 0.03) eV [1]) and the results of *ab initio* calculations (formation energy $(1.93 - 2.02)$ eV [33], 2.07 eV [34]; migration energy 0.65 eV [33], 0.67 eV [34]).

Table II. Calculated formation E^F and migration E^M energies (eV), relaxation volume $V^R(\Omega)$ (Ω – atomic volume) and dipole tensor P_{ij} (eV) for various defect configurations in Fe crystal.

Defect configuration	E^F	E^M	V^R	P_{11}	P_{22}	P_{33}	P_{13}	P_{23}	P_{12}
<110> dumbbell	4.384	0.246	1.480	18.04	18.04	20.39	0	0	4.991
<110> dumbbell saddle point	4.630		1.476	18.88	18.57	18.88	3.257	5.164	5.164
<111> dumbbell	4.627	0.01	1.436	18.27	18.27	18.27	6.365	6.365	6.365
Vacancy	1.920	0.735	-0.140	-1.776	-1.776	-1.776	0	0	0
Vacancy saddle point	2.655		-0.112	-1.428	-1.428	-1.428	-1.684	-1.684	-1.684
Divacancy (2nd nn)	3.63	0.70	-0.36						
The stable di-SIA	7.88	0.17	2.84						

Temperature dependence of vacancy diffusion D^{RW}, D^d and corresponding self diffusion D^* coefficients calculated by MD in temperature range 1000 K < T < 1800 K is presented at Fig. 1 (*a*). Obtained results are described well by Arrhenius equation: $D^{RW}(T) = 13.71 \cdot 10^{-3} e^{-(0.743 \text{ eV})/kT}$ cm^2/s, $D^d(T) = 8.49 \cdot 10^{-3} e^{-(0.733 \text{ eV})/kT}$ cm^2/s, $D^*(T) = 5.35 \cdot 10^{-3} e^{-(0.720 \text{ eV})/kT}$ cm^2/s, k is Boltzmann constant. The analysis of vacancy trajectories has shown that additional diffusion mechanisms are activated at high temperatures, at which the vacancy migrates to the 3rd and the 5th nearest neighbors (nn) positions, besides the ordinary vacancy migration mechanisms to the 1st nn. These two additional mechanisms are sketched out at Fig. 2. Temperature dependences of jump frequencies corresponding to the three observed vacancy migration mechanisms are presented at Fig. 1 (*b*). The approximation of these dependences by Arrhenius equation gives the following values of the activation energies: 0.730 eV, 1.401 eV and 1.664 eV for the jumps to the 1st, 5th and 3rd nn positions, correspondingly. These values agree with the corresponding barriers calculated by MS: 0.735 eV, 1.406 eV, 1.743 eV. Temperature dependences of vacancy correlation factor f_d and corresponding tracer correlation factor f_{tr} are presented at Fig. 3. f_{tr} agree with its theoretical value 0.72722 [31] within the limits of inaccuracy at the temperatures below ~ 1500 K. At higher temperatures some weak systematic decrease is observed. This is apparently concerned with the activation of two mentioned above less energetically favorable migration mechanisms.

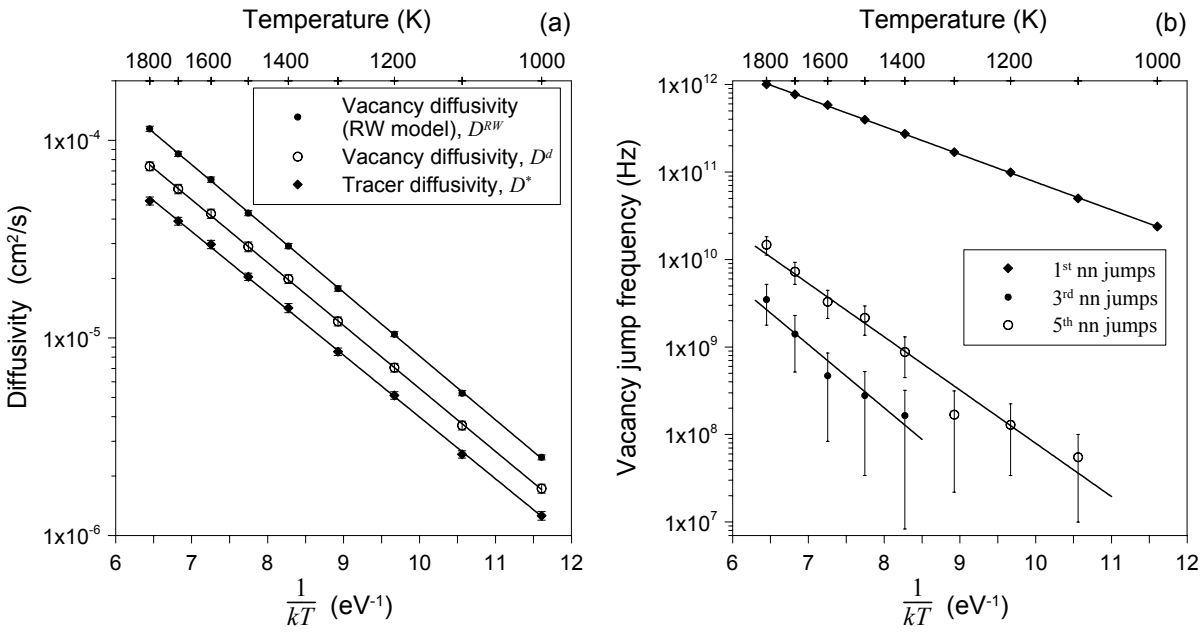

Figure 1. (a) Vacancy diffusion D^{RW}, D^d and self-diffusion D^* coefficients in bcc iron; (b) frequencies of vacancy jumps to the 1st nn, the 3rd nn and the 5th nn positions.

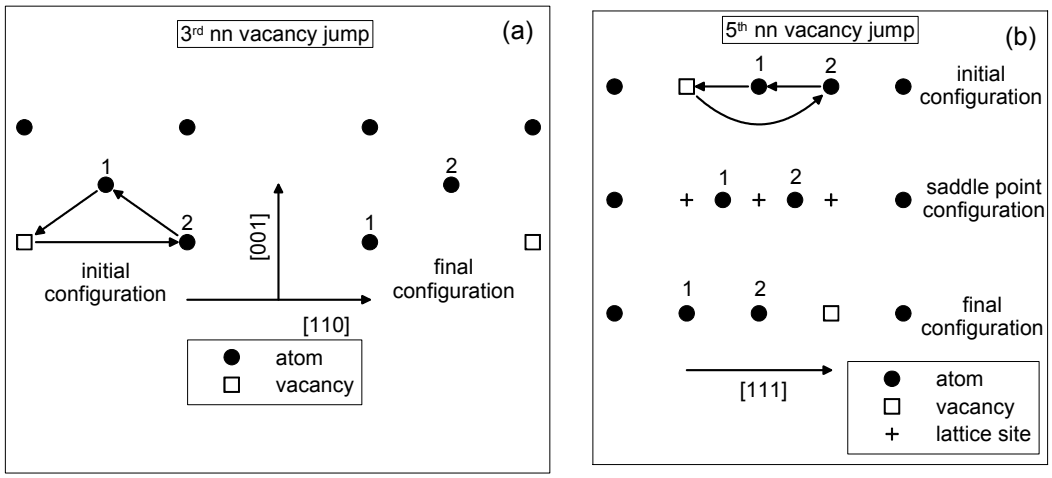

Figure 2. Vacancy migration mechanisms: (a) to the 3rd nn position; (b) to the 5th nn position.

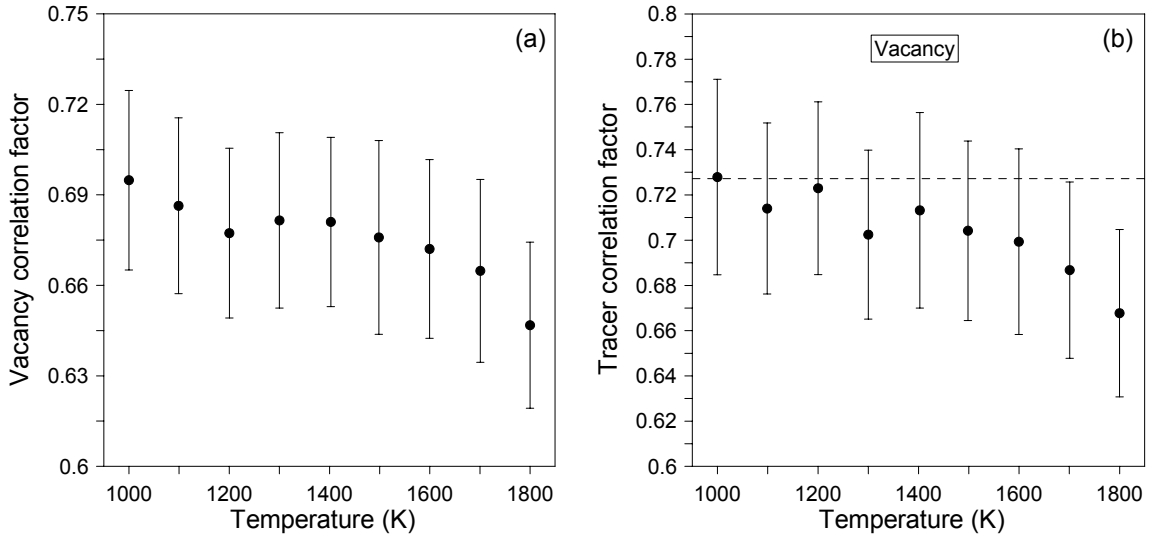

Figure 3. Correlation factors for vacancy in iron: (a) f_d; (b) f_{tr} (dashed line marks the theoretical value f_{tr} = 0.72722 [31] for bcc lattice).

The stable SIA configuration is <110> dumbbell with static migration barrier 0.246 eV in agreement with experimental data [35,36] and ab initio calculations [33,34]. Temperature dependences of SIA diffusion coefficients D^{RW}, D^{D} and corresponding self diffusion coefficient D^{*} calculated by MD in temperature interval 250 K < T < 1800 K are presented at Fig. 4 (*a*). Obtained temperature dependences sufficiently differ from Arrhenius type. Determined from them effective migration energies are ~ (0.22 – 0.23) eV at T < 300 K. These values are close to the calculated values of static energy barriers of <110> dumbbell migration and <110> to <111> dumbbell reorientation processes (0.246 eV and 0.250 eV, respectively) and in agreement with the experimentally measured value ~ 0.25 – 0.3 eV at annealing stage I_E temperature of irradiated specimens [35,36]. The effective migration energy decreases to the value ~ 0.10 eV with the temperature.

The analysis of SIA spatial orientations during the process of diffusion has shown that an SIA has complex migration mechanism at low temperatures. Initially the SIA stays in an <110> dumbbell configuration. Then the SIA migrates to another <110> dumbbell configuration or the SIA reorientation to an <111> dumbbell configuration takes place followed by several (~ 10) fast jumps by crowdion mechanism, after which the SIA returns to an <110> dumbbell configuration. The SIA spends the greatest part of its time at low temperatures in an <110> dumbbell configuration. It follows from these results that, despite the contribution of crowdion mechanism to diffusion, the SIA effective migration energy at low temperatures is determined by the energetic barrier of reorientation from <110> to <111> dumbbell configuration.

The tracer correlation factor f_{tr} is sensitive to the SIA migration mechanism. For pure 1D diffusion f_{tr} = 0. In case of <110> dumbbell migration mechanism, f_{tr} = 0.42 [37]. The value of f_{tr} calculated by MD (Fig. 4 (*b*)) is constant within the limits of inaccuracy through the whole temperature range. Its average equals to 0.27, which is evidence of the complex diffusion mechanism not changing with the temperature.

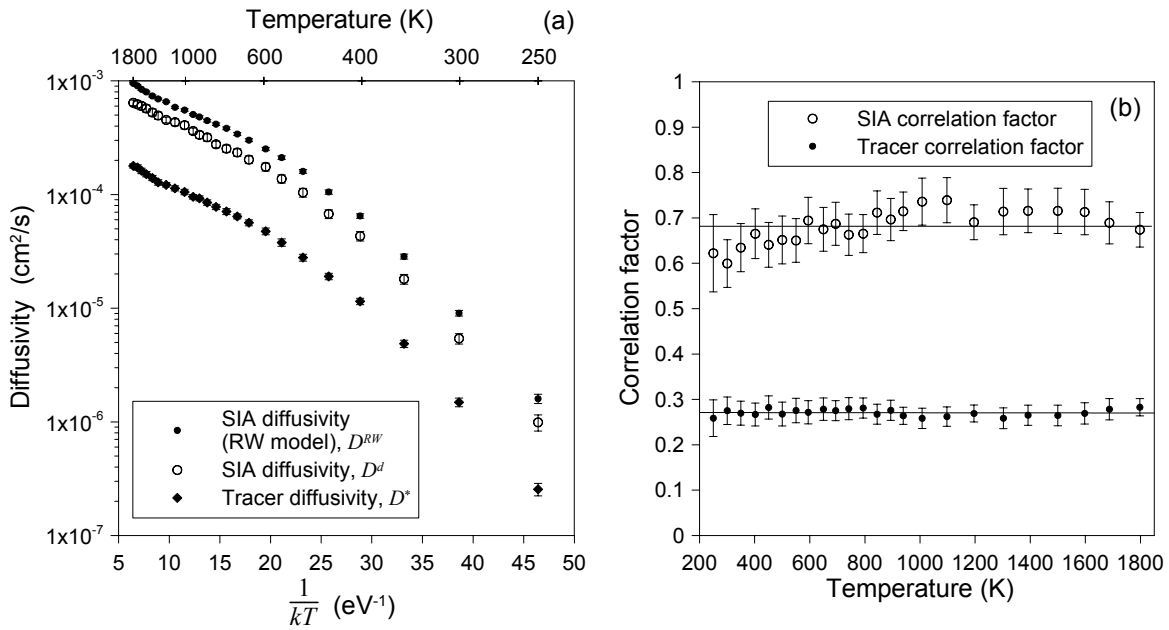

Figure 4. (a) SIA diffusion D^{RW}, D^d and self-diffusion D^* coefficients in bcc iron; (b) SIA f_d and tracer f_{tr} correlation factors (solid lines show the values averaged through the whole temperature range).

5. CONCLUSIONS

1. Calculated vacancy formation energy (2.50 eV) and migration energy (0.48 eV) in vanadium agree well with experimental data and *ab initio* calculations [6,7].

2. The results of computer simulation have shown that the stable SIA configuration in vanadium is <110> dumbbell with the migration energy 0.17 eV. These results are in agreement with the activation energy estimated from annealing stage I_E temperature in vanadium (~ 80 K) [9-11] and with the results of measurements [12]. On this basis the conclusion is made that migration of stable <110> dumbbell takes place at I_E stage. Metastable <111> dumbbell migrates at low temperature ($T < 20$ K) with the activation energy 0.01 eV in agreement with experimental observations [38]. These results do not agree qualitatively with the results of *ab initio* calculations [6,7].

3. Calculated vacancy formation (1.92 eV) and migration (0.735 eV) energy in bcc iron agree well with experimental data [1,32] and *ab initio* calculations [/33,34]. Vacancy activation energy calculated by molecular dynamics (MD) practically coincides with one calculated by molecular statics (MS).

4. Calculations have shown that the stable SIA configuration in iron is <110> dumbbell. This is confirmed by experimental observations [35,36] and *ab initio* calculations [33,34]. MD study of SIA diffusion has shown that SIA migration mechanism is complex and is characterized by superposition of 1D and 3D migration mechanisms. SIA effective migration energy increases

from 0.10 eV to 0.23 eV when the temperature goes down from the melting temperature to 250 K. Indicated tendency shows that SIA migration energy should come to 0.25 eV at the annealing stage I_E temperature (~125 K). This value agrees with the value of the energetic barrier obtained by MS (0.25 eV) and with the experimental measurements [35,36].

ACKNOWLEDGMENTS

The present work was funded by Russian Foundation for Basic Research (project RFBR 05-02-08128ofi-e).

REFERENCES

1. V. A. Romanov, A. B. Sivak, V. M. Chernov, "Crystallographic, energetic and kinetic properties of self-point defects and their clusters in bcc iron," *Voprosy Atomnoy Nauki i Tekhniki, Ser.: Materialovedenie i novye materialy*, **1(66)**, pp.129-232 (2006).
2. K. Maier, M. Peo, B. Saile, H. E. Schaefer, A. Seeger, "High-temperature positron annihilation and vacancy formation in refractory metals," *Philos. Mag. A*, **40**, p. 701 (1979).
3. C. Janot, B. George, P. Delcroix, "Point defects in vanadium investigated by Mössbauer spectroscopy and positron annihilation," *J. Phys. F*, **12**, p. 47 (1982).
4. H. Schultz, in: H. Ullmaier (Ed.), Landolt-Bornstein, New Series, Group III, Vol. 25, Springer, Berlin, (1991).
5. A. Van Veen, H. Eleveld, M. Clement, "Helium impurity interactions in vanadium and niobium," *J. Nucl. Mater.*, **212-215**, p. 287 (1994).
6. S. Han, L. A. Zepeda-Ruiz, G. J. Ackland, R. Car, D. J. Srolovitz, "Self-interstitials in V and Mo," *Phys. Rev. B*, **66**, 220101 (2002).
7. D. Nguyen-Manh, A. P. Horsfield, S. L. Dudarev, "Self-interstitial atom defects in bcc transition metals: group-specific trends," *Phys. Rev. B*, **73**, 020101(R) (2006).
8. J. H. Evans, EURATOM/UKAEA Fusion Report No. 499 (2003).
9. B. S. Brown, T. H. Blewitt, T. L. Scott, A. C. Klank, "Low-temperature fast-neutron radiation damage studies in superconducting materials," *J. Nucl. Mater.*, **52**, p. 215 (1974).
10. S. Takamura, S. Okuda, "Recovery of fast neutron irradiated niobium and vanadium at low temperature," *J. Phys. Soc. Jpn.*, **35**, p. 750 (1973).
11. C. E. Klabunde, J. K. Redman, A. L. Sonthern, R. R. Coltman, "Thermal and fission neutron damage in vanadium," *Phys. Stat. Sol. A*, **21**, p. 303 (1974).
12. T. Hayashi, K. Fukumoto, H. Matsui, "Study of point defect behaviors in vanadium and its alloys by using HVEM," *J. Nucl. Mater.*, **283-287**, p. 234 (2000).
13. V. A. Romanov, V. M. Chernov, A. B. Sivak, "Energetic, Kinetic and Crystallographic Characteristics of Self-point Defects in Vanadium," *Abstracts of The 8th IEA International Workshop on Vanadium Alloys for Fusion Applications*, St. Petersburg, Russia, June 5-6, 2006, p. 29 (2006).
14. M. W. Finnis, J. E. Sinclair, "A simple N-body potential for transition metals," *Philos. Mag. A*, **50**, p. 45 (1984).
15. J. F. Ziegler, J. P. Biersack, U. Littmark, "The stopping and range of ions in solids," *The stopping and range of ions in matter*, vol. 1, J. F. Ziegler (ed.), Pergamon, New York (1985).

16. D. J. Bolef, R. E. Smith, J. G. Miller, "Elastic properties of vanadium. I. Temperature dependence of the elastic constants and the thermal expansion," *Phys. Rev. B*, **3**, p. 4100 (1971).
17. C. Kittel, *Introduction to Solid State Physics*, 5th ed., Wiley, New York, USA (1976).
18. V. N. Zharkov, V. A. Kalinin, *Uravneniya sostoyaniya tverdykh tel pri vysokikh davleniyakh i temperaturakh*, Nauka, Moscow, USSR (1968) (in Russian).
19. *High-Velocity Impact Phenomena*, ed. by R. Kinslow, Academic Press, New York and London, p. 538 (1970).
20. R. F. Peart, "Diffusion of V^{48} and Fe^{59} in vanadium," *J. Phys. Chem. Solids*, **26**, p. 1853 (1965).
21. T. S. Lundy, C. J. McHarque, "Diffusion of V^{48} in vanadium," *Trans. Met. Soc. AIME*, **233**, p. 243 (1965).
22. J. Pelleg, "Self diffusion in vanadium single crystals," *Philos. Mag.*, **29**, p. 383 (1974).
23. V. Segel, J. Pelleg, "Vanadium diffusion in V-Co dilute alloys," *Philos.Mag. A*, **76**, p. 1203 (1997).
24. M. P. Macht, G. Frohberg, H. Wever, "Selbstdiffusion von vanadium," *Z. Metallk.*, **70**, p. 209 (1979).
25. D. Ablitzer, J. P. Haeussler, K. V. Sathyaraj, "Vanadium self-diffusion in pure vanadium and in dilute vanadium-iron and vanadium-tantalum alloys," *Philos. Mag. A*, **47**, p. 515 (1983).
26. H. R. Schober and K. W. Ingle, "Calculation of relaxation volumes, dipole tensors and Kanzaki forces for point defects," *J. Phys. F: Metal Phys.*, **10**, pp. 575 -581 (1980).
27. G. Leibfried, N. Breuer, *Point defects in metals* I, Springer-Verlag, Berlin, Germany (1978).
28. L. Verlet, "Computer "experiments" on classical fluids. I. Thermodynamical properties of Lennard-Jones molecules," *Phys. Rev.*, **159**, p. 98 (1967).
29. Yu. N. Osetsky, "Atomistic study of diffusional mass transport in metals," *Defect and Diffusion Forum*, **188-190**, pp.71-92 (2001).
30. M. W. Guinan, R. N. Stuart, R. J. Borg, "Fully dynamic computer simulation of self-interstitial diffusion in tungsten," *Phys. Rev. B*, **15**, p. 699 (1977).
31. J. R. Manning, *Diffusion kinetics for atoms in crystals*, D. Van Nostrand Company, Toronto, Canada (1968).
32. L. De Schepper, D. Segers, L. Dorikens-Vanpraet, M. Dorikens, G. Knuyt, L. M Stals, P. Moser, "Positron annihilation on pure and carbon-doped α-iron in thermal equilibrium," *Phys. Rev. B*, **27**, pp.5257-5269 (1983).
33. C. Domain, C.S. Becquart, "Ab initio calculations of defects in Fe and dilute Fe-Cu alloys," *Phys. Rev. B*, **65**, 024103 (2002).
34. C.-C. Fu, F. Willaime, P. Ordejon, "Stability and mobility of mono- and di-interstitials in α-Fe", *Phys. Rev. Lett.*, **92**, 175503 (2004).
35. V. Hivert, R. Pichon, H. Bilder, P. Bichon, J. Verdone, D. Dautreppe, and P. Moser, "Internal friction in low temperature irradiated bcc metals," *J. Phys. Chem. Sol.*, **31**, pp. 1843-1855 (1970).
36. H. E. Schaffer, D. Butteweg, W. Dander, "Defects in High Purity Iron after 27 K electron irradiation," *Proceeding of International Conference on Fundamental Aspects of Radiation Damage in Metals*, Gatlinburg, 1975, p. 463 (1975).
37. A. R. Allnatt, A. B. Lidiard, *Atomic transport in solids*, Cambridge University Press, p. 359 (1993).
38. R. R. Coltman, C. E. Klabunde, J. K. Redman, J. M. Villiams, *Radiat. Eff.*, **24**, p. 69 (1975).

APPENDIX A

Table A.I. Coefficients a_k (eV/Å^k) of constituent polynomials $\sum_{k=0}^{5} a_k r^k$ of $\varphi(r)$ for V.

Range, Å	a_0	a_1	a_2	a_3	a_4	a_5
[1.1, 1.68265]	3939.000592	-11646.178368	14279.880970	-8951.709303	2841.797566	-363.219173
[1.68265, 2.2653]	2309.324943	-5247.184510	4824.080686	-2232.695804	518.545945	-48.246223
[2.2653, 2.4]	-9645.768516	20936.258309	-18112.789376	7813.110123	-1681.228810	144.419295
[2.4, r_1]	978.549717	-1695.718889	1162.175689	-391.035348	63.991085	-4.017606
[r_1, r_2]	18.995072	-129.576761	169.652405	-89.945914	21.414908	-1.907382
[r_2, 3.0702]	756.649294	-1033.921783	558.720049	-149.312427	19.746212	-1.035644
[3.0702, 3.12]	542.664755	-674.061616	316.889539	-68.132145	6.132516	-0.123214
[3.12, 3.2]	284177.464822	-449900.422334	284874.436084	-90180.144083	14272.107201	-903.387433
[3.2, 4.074]	938.852807	-1250.073989	661.707699	-174.210004	22.827429	-1.191662

Table A.II. Parameters of function (2).

a, eV/Å^n	-0.250566	b, eV/Å^m	0.282631	n	3	m	4

Table A.III. Coefficients b_k (eV^2/Å^k) of constituent polynomials $\sum_{k=0}^{5} b_k r^k$ of $\rho(r)$ for V.

Range, Å	b_0	b_1	b_2	b_3	b_4	b_5
[r_2, 3.7]	81.320229	-67.596452	17.745451	-0.616599	-0.383204	0.041705
[3.7, 4.074]	-636.646443	861.846541	-462.611713	123.251701	-16.317034	0.859472